Effect of Microstructural Evolution on the Creep Properties of Carbon and Boron Modified SX Alloy RR2072

D.H. Kim [a,b], C.Y. Jo [a], S.W. Nam [b], Y.S. Yoo [a], S.J. Choe [c], and C.N. Jones [d]

[a] *Department of Materials Processing, Korea Institute of Machinery and Materials, 66 Sangnam-dong, Changwon, Gyeongnam 641-010, Korea*
[b] *Department of Materials Science and Engineering, Korea Advanced Institute of Science and Technology, 373-1 Guseong-dong, Yuseong-gu, Daejeon 305-701, Korea*
[c] *Iljin Electric Co., Ltd., 112-83 Annyung-ri, Taean-eup, Hwaseong, Gyeonggi 445-976, Korea*
[d] *Rolls-Royce plc, PO Box 31, Derby, DE24 8BJ, UK*

(Received September 13, 2002)

ABSTRACT

The relationship between microstructural evolution and creep properties of carbon and boron modified single crystal superalloy RR2072* has been investigated. Three kinds of single crystal specimen were prepared for comparative study; fully solutionized base alloy, partially solutionized base alloy, and the carbon and boron modified alloy. Creep and thermal exposure tests of the single crystal specimens were performed at 950 °C and 1050 °C. Addition of carbon and boron to the base alloy RR2072 made it difficult to bring the existing phases into solution. Partial solutionizing of the existing phases decreased the creep resistance of the single crystal. However, carbon and boron retarded precipitation of the σ phase under both creep and thermal exposure conditions. Owing to the delayed precipitation of σ phase, the creep properties of the modified alloy were similar to those of the base alloy.

1. INTRODUCTION

To improve the efficiency of gas turbines, single crystal casting has been adapted in the production of high temperature components, such as turbine blades and vanes /1/. Due to their geometrical complexity, the air-cooled turbine vanes are susceptible to grain defects during single crystal casting /2/.

In order to mitigate the grain problem of the air-cooled single crystal vanes, grain boundary strengthening by the addition of minor elements such as carbon, boron, hafnium and zirconium has been the subject of several researches /3,4,5/. The studies are focused on the improvement of the grain misorientation allowance through the grain boundary strengthening. Especially, carbon and boron were mainly considered to strengthen grain boundaries generated as a defect during single crystal casting. Because the addition of those elements makes it difficult to bring the existing phases into matrix γ during solution treatment, it may deteriorate high temperature properties of the alloy /6,7/. Therefore, much attention has to be paid to determine the optimum amount of those minor elements not only to strengthen the grain boundary but also to minimize the loss of the characteristics of single crystal.

In the present study, the effect of carbon and boron on the creep properties of single crystal RR2072* has been investigated.

* *Experimental alloy of Rolls-Royce plc.

2. EXPERIMENTAL PROCEDURE

Table 1 shows the chemical compositions of the experimental alloys. The base alloy (RR2072, hereinafter: BASE alloy) is free from carbon and boron. The carbon and boron modified alloy (hereinafter: MOD E alloy) contains 0.05 wt% C and 0.010 wt% B on the base of the BASE alloy composition. The MOD E alloy also contains 0.05 wt% more Hf than the BASE alloy. The master ingots of the BASE and MOD E alloy have been prepared by vacuum induction melting.

The [001] oriented single crystal bars of the alloys were cast in the modified Bridgeman furnace. The single crystal bars were 15 mm in diameter and 170 mm in length.

The single crystal bars were heat treated as shown in Table 2. The heat treatment cycles consisted of solution and double aging treatments. To prevent incipient melting, solution treatment of the MOD E alloy was carried out at 25 °C lower than that of the BASE alloy. The BASE specimen solutioned at the same solution temperature with the MOD E alloy (hereinafter: the partially solutionized BASE specimen) was also prepared for comparison. The heat-treated bars were machined to be creep specimens with 27mm gauge length and 6mm diameter.

Constant load creep tests were conducted for the heat-treated single crystal specimens at 950 °C / 290 MPa and at 1050 °C / 165 MPa. The creep strain was measured by LVDT (linear variable differential transformer) through measuring jigs fixed at the specimen shoulders.

Thermal exposure tests were carried out at 950 °C and at 1050 °C for 100 hours to understand the microstructural evolution of the alloys. Thermal exposure tests for the MOD E alloy were continued up to 1000 hours.

Metallographic observations were carried out with the optical microscope and scanning electron microscope (JSM 5800). Metallographic specimens were prepared by mechanical polishing and etched by Kalling's reagent.

3. RESULTS AND DISCUSSION

Microstructure of the heat-treated specimens is displayed in Fig. 1. Microstructure of the BASE specimen solutionized at 1320 °C consists of uniformly dispersed γ′ with 0.5 μm in size and the γ matrix. Since the γ/γ′ eutectic and primary γ′ phases were completely dissolved into the matrix γ during solution treatment at 1320 °C, the heat-treated BASE specimen showed the uniform microstructure. However, the relatively low temperature (1295 °C) solutionizing adapted to the MOD E specimen to prevent incipient melting resulted in incomplete dissolution of γ/γ′ eutectic and primary γ′ phases. Because carbon is present in the alloy, the specimen also has MC carbide that was identified as Ta-rich carbide through SEM-EDS analysis.

The role of boron in the equiaxed superalloy is generally known to strengthen the grain boundaries through its segregation to the grain boundaries /8/.

Table 2
Heat treatment cycles of single crystal specimen

Alloy	Solution treatment	Aging
BASE	1320 °C / 6 hrs / GFQ*	1140 °C / 2 hrs / GFQ* + 870 °C / 16 hrs / AC**
MOD E	1295 °C / 6 hrs / GFQ*	

*GFQ: gas fan quench
**AC: air cool

Table 1
Chemical composition of RR2072 BASE and MOD E alloy (in wt%)

Element	Co	Cr	Mo	W	Re	Al	Ti	Ta	Nb	C	B	Hf	Ni
BASE	4.0	6.0	3.3	1.9	3.0	6.2	0.4	5.95	0.8	-	-	0.10	Bal.
MOD E	4.0	6.0	3.3	1.9	3.0	6.2	0.4	5.95	0.8	0.05	0.010	0.15	Bal.

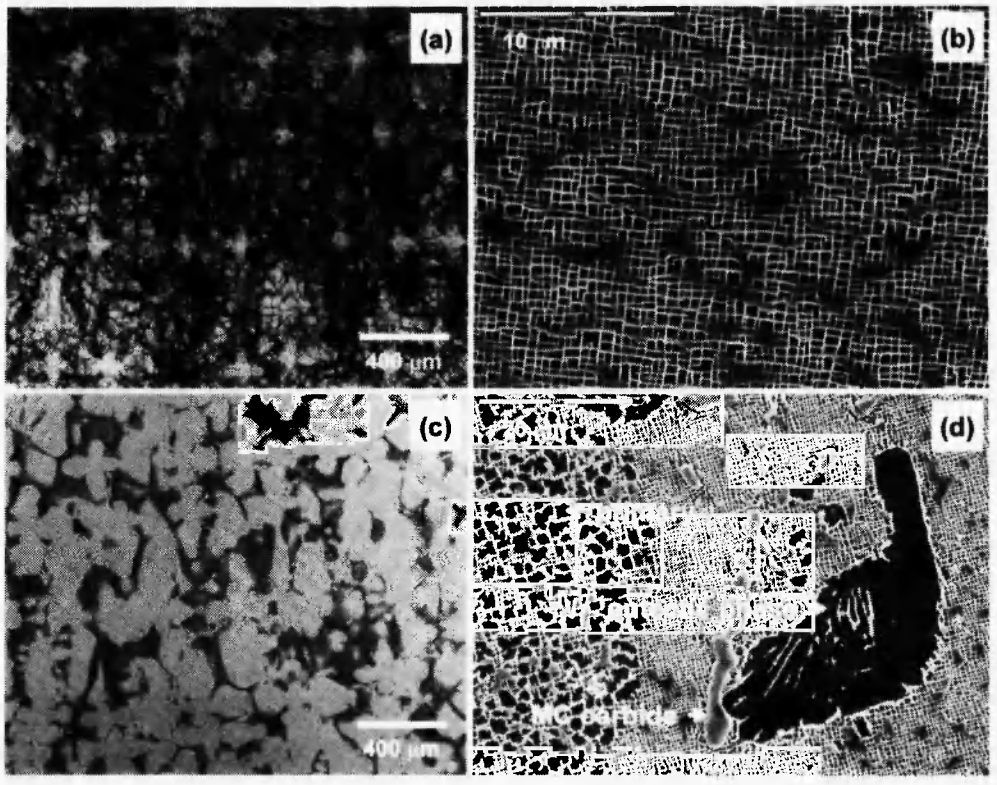

Fig. 1: Micrographs of heat-treated BASE alloy [(a), (b)] and MOD E alloy [(c), (d)]. (a) and (c) are optical micrographs, and (b) and (d) are SEM micrographs.

However, boron is expected to exist in the interdendritic regions in the single crystal because there is no grain boundary /9/. Although boron may precipitate as borides, no evidence of borides was observed in this investigation owing to minor addition of boron.

Creep curves of the BASE and MOD E alloy specimens were plotted in Fig. 2. The minimum creep rate was calculated from the curves and listed in Table 3 in conjunction with the rupture lives and rupture elongations of the specimens. The results at 950°C/290 MPa showed that the BASE specimen had relatively low minimum creep rate and the MOD E specimen had relatively long rupture life. At 1050 °C / 165 MPa fully solutioned BASE alloy and MOD E alloy showed

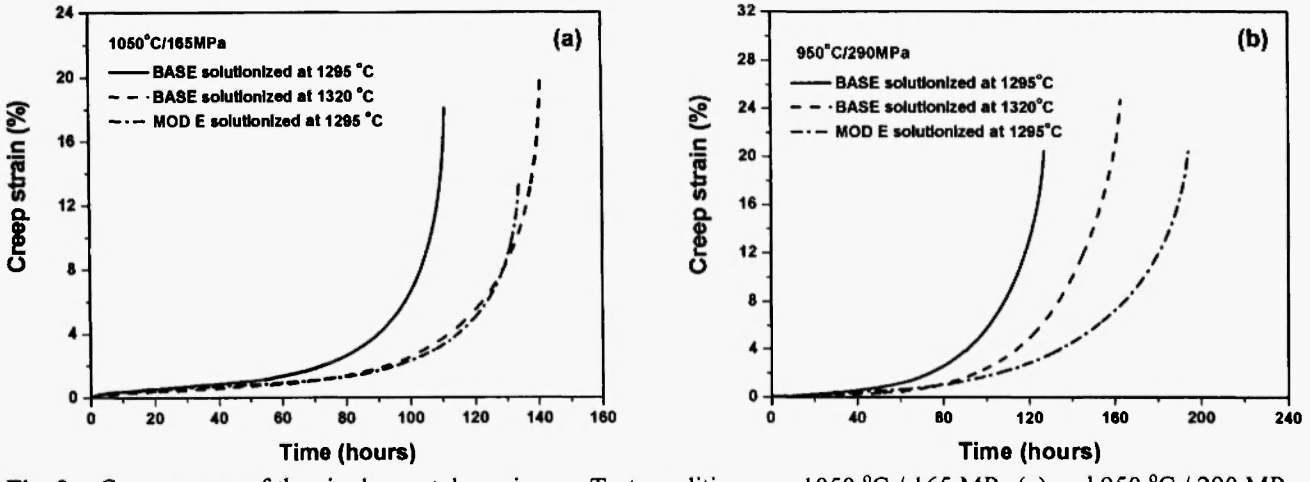

Fig. 2: Creep curves of the single crystal specimens. Test conditions are 1050 °C / 165 MPa (a) and 950 °C / 290 MPa (b).

Table 3
Creep properties of RR2072 BASE and MOD E alloy single crystals

Test Condition	Specimen	Minimum creep rate (X 10^{-8}/sec)	Rupture life (hours)	Rupture elongation (%)
1050 °C/ 165 MPa	BASE*	2.641	140.9	22.8
	BASE**	4.163	110.9	19.5
	MOD E	2.725	133.9	14.0
950 °C/ 290 MPa	BASE*	2.263	162.9	30.2
	BASE**	4.052	127.1	21.7
	MOD E	2.766	194.2	21.7

* BASE single crystal fully solutionized at 1320 °C
** BASE single crystal partially solutionized at 1295 °C

similar minimum creep rate and rupture life. The partially solutionized BASE specimen has relatively high minimum creep rate and short rupture life at both test conditions.

It has been reported that uniform distribution of γ′ particles of about 0.5 μm in size decreased minimum creep rate and increased rupture life of nickel base single crystal superalloy CMSX-2 /10/. It was found that the creep resistance of the alloy improved through the formation of well-arrayed rafts which effectively suppressed climb of dislocation.

The reduced creep resistance of the partially solutionized BASE specimen seems to be attributed to the microstructural inhomogeneity. However, the MOD E specimen has similar minimum creep rate and good resistance to creep deformation in the tertiary stage compared with the fully solutionized BASE specimen. It should be noted that the creep properties of MOD E specimen exceed the expectation that they would be similar to those of the partially solutionized BASE specimen, since the microstructure of MOD E specimen is inhomogeneous like that of the partially solutionized BASE specimen.

The micrographs of the crept BASE and MOD E specimens are displayed in Fig. 3. They were taken in the dendrite arm area on the longitudinal section 5 mm apart from the fracture surface. All the specimens showed rafted γ′ structure. The gray phase is matrix γ and the dark phase is precipitate γ′. The rod shaped white precipitates were identified as σ phase enriched by Re, Cr, Mo, W and Co /11/. The σ phase in the BASE specimen is fairly uniformly distributed compared with those of the MOD E specimen. Distribution of σ phase in the partially solutionized BASE specimen was similar to that of the fully solutionized BASE specimen. The σ phase in the MOD E specimen became needle or plate-like after 1050 °C / 165 MPa creep test.

The rafted structure of the MOD E specimen is relatively well aligned at both test conditions. Isolation of the matrix γ like those of the BASE specimen [see Fig. 3 (a) – (d)] seems to be typical morphology in the crept single crystal specimens. The isolation of matrix γ is attributed to severe deformation at the tertiary stage /12/. It is noted that the crept MOD E specimen has well aligned raft structure and has inhomogeneous

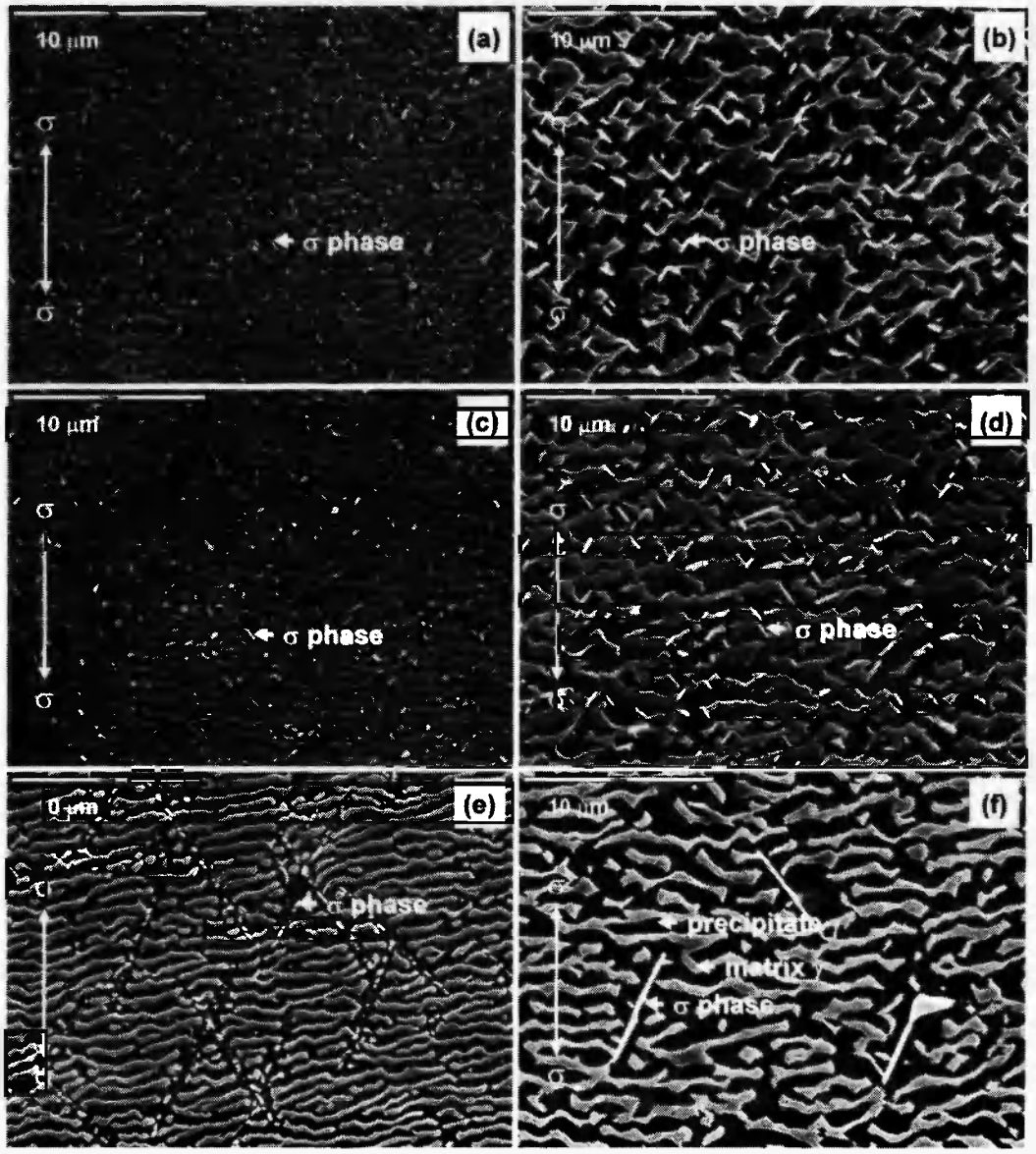

Fig. 3: Micrographs of dendrite arm area of crept single crystals. Left column was crept at 950 °C / 290 MPa, and right column was crept at 1050 °C / 165 MPa.
(a), (b) BASE specimen fully solutionized at 1320 °C,
(c), (d) BASE specimen partially solutionized at 1295 °C,
(e), (f) MOD E specimen solutionized at 1295 °C.

distribution of σ phase.

Microstructural observations in the interdendritic region of the crept partially solutionized BASE and MOD E specimen were also carried out and summarized in Fig. 4. The observed area was the interdendritic region 5 mm apart from the fracture surface. The shapes of primary γ′ in both specimens are elongated normal to the direction of applied stress. The σ phase also appears in the partially solutionized BASE specimens [Fig. 4 (a) and (b)], but does not appear in the MOD E specimen [Fig. 4 (c) and (d)]. In the case of the BASE specimen solutionized at 1320 °C, there was no interdendritic region including the coarse primary γ′ phases because the phases were completely dissolved into the matrix γ

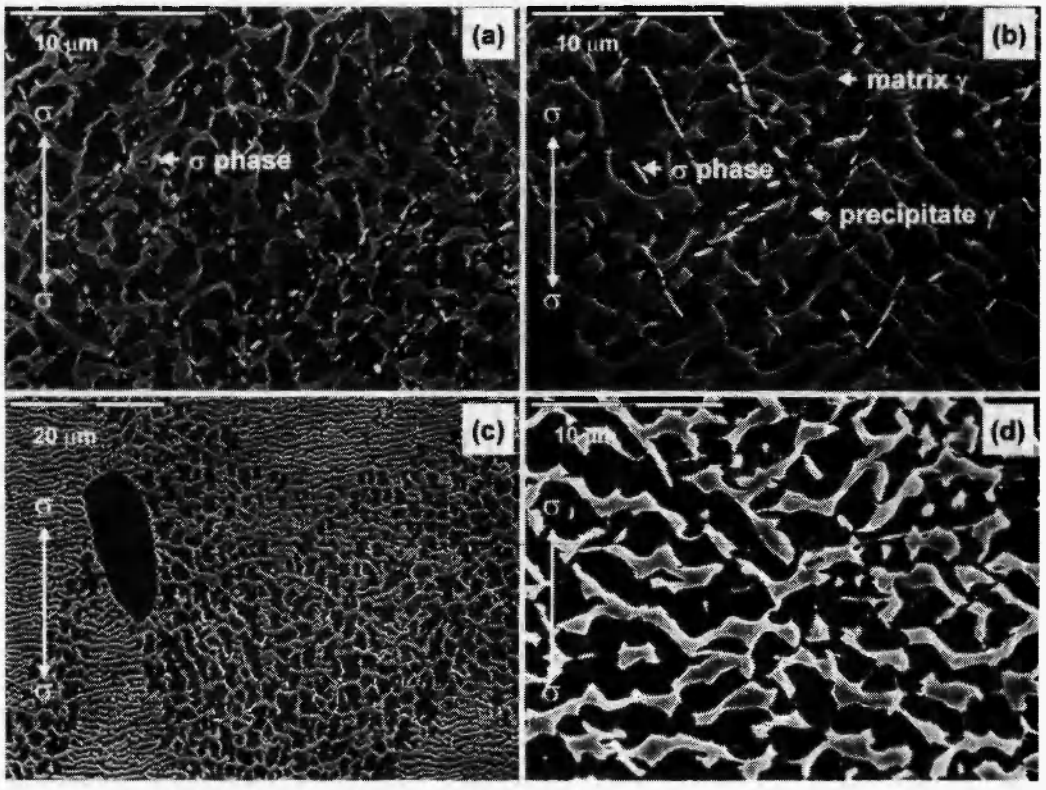

Fig. 4: Micrographs of interdendritic area of crept single crystals. Left column was crept at 950 °C / 290 MPa, and right column was crept at 1050 °C / 165 MPa.
(a), (b) BASE specimen partially solutionized at 1295 °C,
(c), (d) MOD E specimen solutionized at 1295 °C.

during solution treatment. From the above results, it is postulated that precipitation behavior of the σ phase is different for each alloy.

Thermal exposure tests were carried out at the creep temperatures to compare the precipitation behavior of the σ phase between the two alloys without stress. Fig. 5 shows the micrographs taken in the middle of the dendrite arms that were exposed at 950 °C and 1050 °C for 100 hours. Little or no growth of γ′ particles was observed in the specimens exposed at 1050 °C for 100 hours, and detectable growth was not found in the specimens exposed at 950 °C for 100 hours. The σ phase was observed in the BASE specimens after exposure at 950 °C and 1050 °C for 100 hours. However, the σ phase did not form in the MOD E specimen even at the same thermal exposure conditions.

Precipitation behavior of the σ phase in the interdendritic region was similar to that observed in the middle of the dendritic arms as shown in Fig. 6. But the amount in the interdendritic region of the partially solutionized BASE specimen was relatively low. In the case of the BASE specimen solutionized at 1320 °C, there was no interdendritic region including the coarse primary γ′ phases because the phases were completely dissolved into the matrix γ during solution treatment. In terms of the σ phase precipitation the MOD E alloy exposed at 950 °C for 1000 hours was analogous to the BASE alloy for 100 hours at the same temperature as shown in Fig. 7 (a). In the interdendritic regions of the MOD E specimen exposed at 950 °C for 1000 hours, the σ phase exists in the vicinity of the MC carbide [Fig. 7 (b)], but does not exist in the carbide free region [Fig.

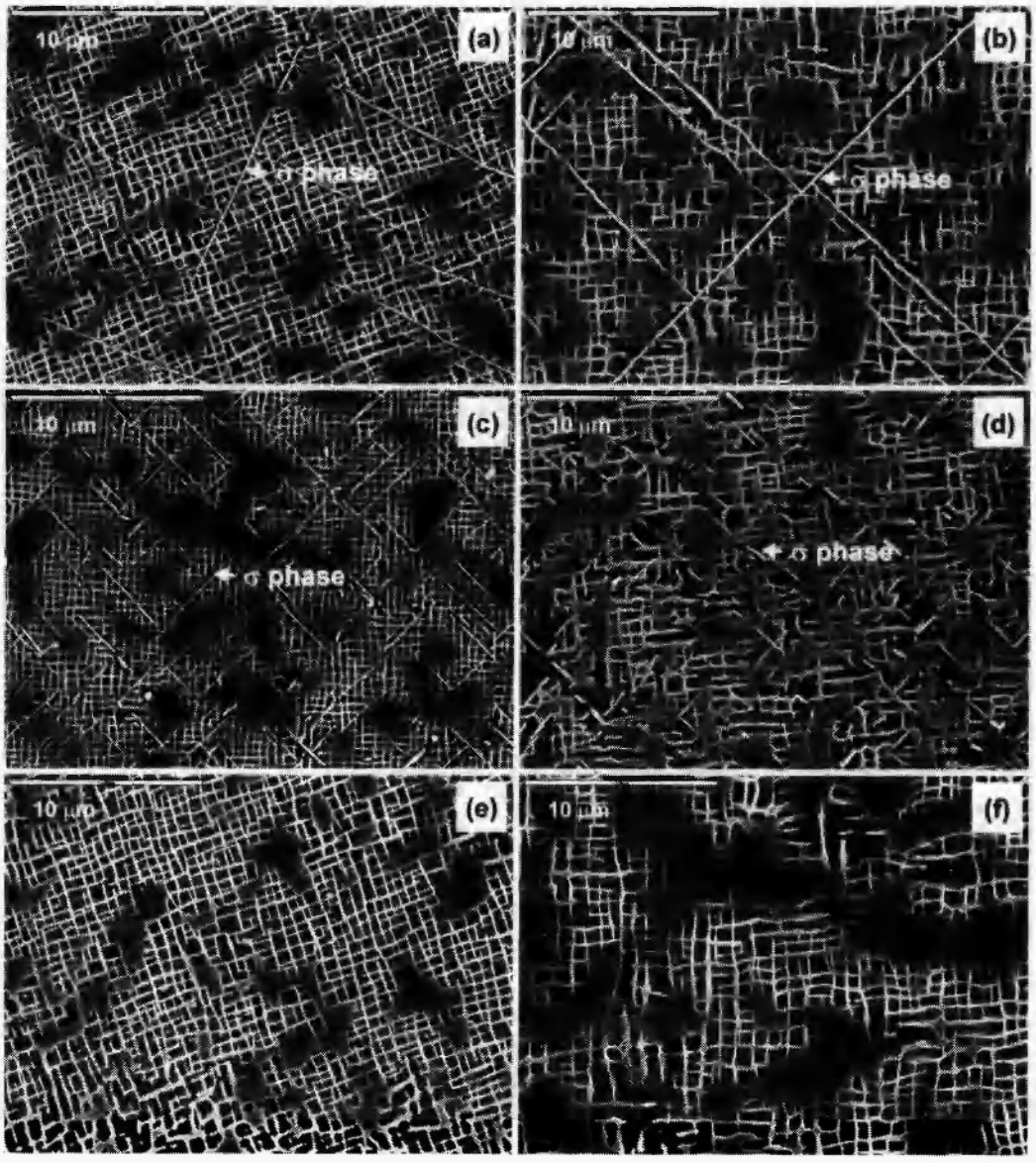

Fig. 5: Micrographs of dendrite arm area of exposed single crystals. Left column was exposed at 950 °C / 100 hours, and right column was exposed at 1050 °C / 100 hours.
(a), (b) BASE specimen fully solutionized at 1320 °C,
(c), (d) BASE specimen partially solutionized at 1295 °C,
(e), (f) MOD E specimen solutionized at 1295 °C.

7 (c)].

From the above results, a correlation between creep properties and microstructural evolution can be made as follows. To prevent incipient melting in the interdendritic regions, the MOD E specimen was heat treated at 25 °C lower than the solutionizing temperature of the BASE specimen. Therefore, the coarse primary γ′ and γ/γ′ eutectic phase still remains in the interdendritic region of the MOD E specimen after heat treatment (see Fig. 1). A little high minimum creep rate of the MOD E specimen is supposed to be related to the local deformation in the interdendritic region due to the microstructural inhomogeneity. However, the minimum creep rate of the MOD E was much lower than that of

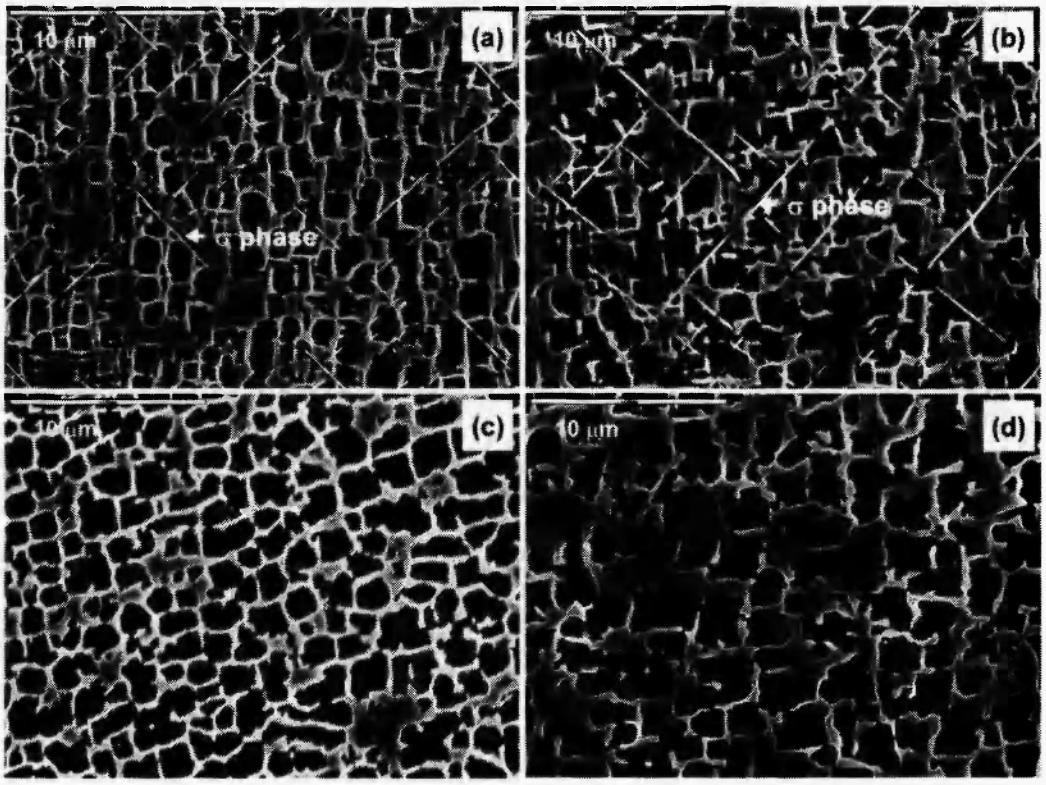

Fig. 6: Micrographs of interdendritic region of exposed single crystals. Left column was exposed at 950 °C / 100 hours, and right column was exposed at 1050 °C / 100 hours.
(a), (b) BASE specimen partially solutionized at 1295 °C,
(c), (d) MOD E specimen solutionized at 1295 °C.

the partially solutionized BASE specimen whose microstructure was similar to that of the MOD E specimen. It means that there is a positive contribution of carbon and boron to the creep resistance of the RR2072 single crystal specimen.

Microstructural observation on the crept specimens showed the difference of raft structure and σ phase precipitation. It is known that, in the nickel base superalloy, the σ phase precipitation weakens the matrix γ due to consuming the solid solution strengthening elements /13/. EDS analysis showed that the σ phase of the BASE and the MOD E specimens contained Cr, Mo, W, Co, as well as much of Re /11/. Thermal exposure tests revealed that the BASE specimen was relatively sensitive to the precipitation of σ phase. Therefore, the relatively low tertiary creep rate of the MOD E specimen can be related to the precipitation behavior of the σ phase. In the MOD E specimen exposed at 950 °C for 1000 hours, the σ phase was precipitated in the middle of dendritic arms and in the vicinity of the MC carbides of the interdendritic regions. The phase was not observed in the carbide free region of the interdendritic regions. The precipitation of the σ phase in the vicinity of the carbide would be caused by the decomposition of the MC carbide at high temperature. It is generally known that MC carbide generates $M_{23}C_6$ with γ′ through reaction with matrix γ. $M_{23}C_6$ carbide is prone to transform to the σ phase due to similar crystal structure /14/. The reaction consumes the σ forming elements such as Cr and Mo to generate $M_{23}C_6$. The interdendritic region normally contains small amounts of Mo and Cr compared to the dendritic arm. Therefore, the σ phase precipitation would be difficult in the carbide free interdendritic regions.

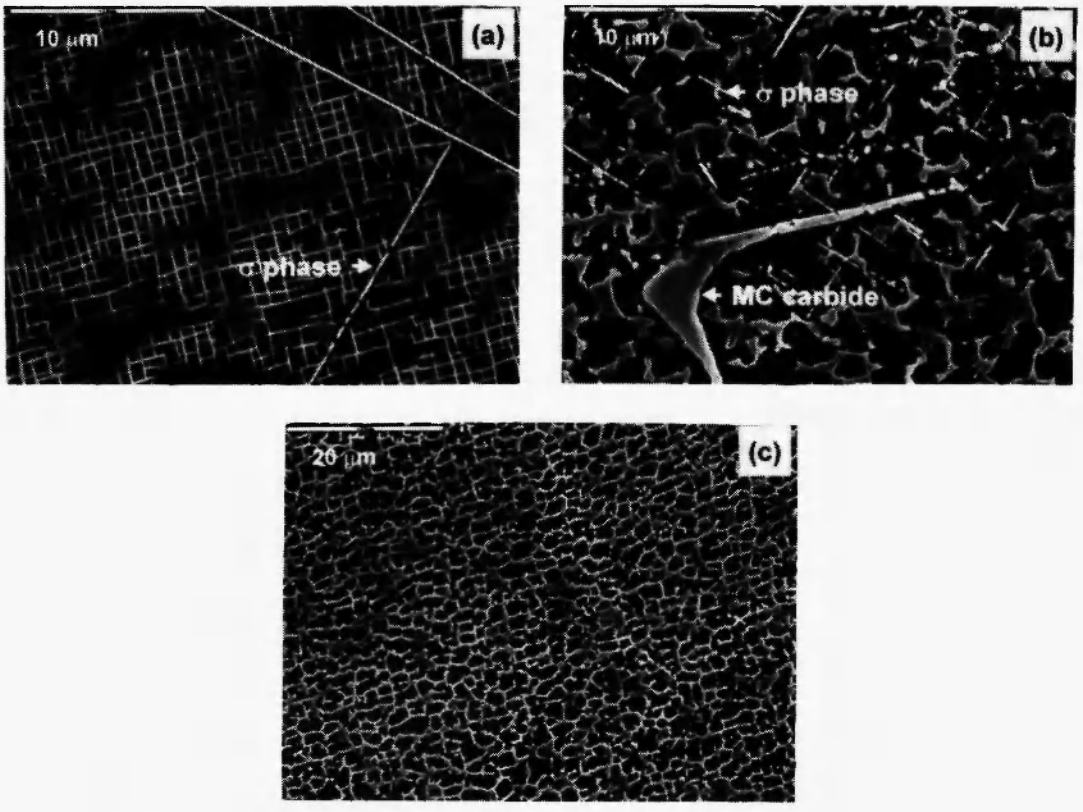

Fig. 7: Micrographs of MOD E single crystal exposed at 950 °C / 1000 hours.
(a) dendrite arm area, (b) interdendritic region including carbide,
(c) carbide free interdendritic region.

4. CONCLUSION

Since minor addition of carbon and boron made it difficult to bring the existing phases into solution in the nickel base single crystal superalloy RR2072, the single crystal of modified alloy had a smaller minimum creep rate than that of the base alloy. In the modified alloy, however, carbon and boron retards precipitation of the σ phase under both creep and thermal exposure conditions. Owing to the delayed precipitation of σ phase, the modified alloy has similar creep lives to the base alloy. It is the positive contribution of carbon and boron on the creep properties of nickel base single crystal superalloy RR2072.

REFERENCES

1. R.W. Broomfield, D.A. Ford, H.K. Bhangu, M.C. Thomas, D.J. Frasier, P.S. Burkholder, K. Harris, G.L. Erickson, and J.B. Wahl, *ASME paper*, 97-GT-117, 1997.
2. K. Harris and J.B. Wahl, *PARSONS 2000 Advanced Materials for 21st Century Turbines and Power Plant*, A. Strang, W.M. Banks, R.D. Conroy, G.M. McColvin, J.C. Neal and S. Simpson (Eds.), IOM Communications Ltd., Cambridge, UK, **II**, 2000; p.832.
3. E.W. Ross, C.S. Wukusick and W.T. King, *US patent* 5399313, 1995.

4. H. Tamaki, A. Yoshinari, A. Okayama and S. Nakamura, *Superalloys 2000*, T.M. Pollock, R.D. Kissinger, R.R. Bowman, K.A. Green, M. McLean, S.L. Olson, and J.J. Schirra (Eds.), TMS, Warrendale, PA, USA, 2000; p.757.
5. P.S. Burkholder, M.C. Thomas, R. Helmink, D.J. Fraiser, K. Harris, and J.B. Wahl, *ASME paper*, 99-GT-379, 1999.
6. P. Caron and T. Khan, *Materials for Advanced Power Engineering 1998*, J. Lecomte-Beckers, F. Schubert and P.J. Ennis (Eds.), Forschungszentrum Jülich GmbH, Jülich, Germany, **5**, part II, 1998; p.897.
7. Q.Z. Chen, N. Jones, D.M. Knowles, *Acta Mater*, **50**, 1095 (2002).
8. R.T. Holt and W. Wallace, *Int. Metals Rev.*, **203**, 1 (1976).
9. J.S. Jang, C.H. Han, Y.K. Kim, and C.H. Lee, *Proc. of the Symp. on Nuclear Materials and Fuel 2000*, J.H. Hong, W.S. Ryu, M.S. Yang, and J.W. Lee (Eds.), Korea Atomic Energy Research Institute, Taejon, Korea, 2000; p.446.
10. P. Caron and T. Khan, *Mater. Sci. Eng.*, **61**, 173 (1983).
11. Q.Z. Chen and D.M. Knowles, *Metall. Mater. Trans. A*, **33**A, 1319 (2002).
12. R.A. MacKay and L.J. Ebert, *Metall. Trans. A*, **16A**, 1969 (1985).
13. C.T. Sims, *Superalloys II*, C.T. Sims, N.S. Stoloff and W.C. Hagel (Eds.), John Wiley & Sons, New York, USA, 1987; p.224.
14. E.W. Ross and C.T. Sims, *Superalloys II*, C.T. Sims, N.S. Stoloff and W.C. Hagel (Eds.), John Wiley & Sons, New York, USA, 1987; p.118.